Mechanical and thermal characterization of an epoxy foam as thermal layer insulation for a glass fiber reinforced polymer

JOURNAL OF Applied Polymer SCIENCE

Mechanical and thermal characterization of an epoxy foam as thermal layer insulation for a glass fiber reinforced polymer

M. Cavasin,[1,2] S. Giannis,[1†] M. Salvo,[2] V. Casalegno,[2] M. Sangermano[2]

[1]Element Materials Technology, Wilbury Way, Hitchin, SG4 0TW, United Kingdom

[2]Department of Applied Science and Technology (DISAT), Politecnico di Torino, Torino, 10129, Italy

Correspondence to: M. Sangermano (E-mail: marco.sangermano@polito.it)

ABSTRACT: We have investigated the formulations and curing parameters to obtain an epoxy foam to be used as thermal insulator layer for a glass fiber reinforced polymer (GFRP). A relevant decrease (50%) of the apparent density of the foam was achieved by adding up to 5 wt % of foaming agent without affecting the glass-transition temperature (T_g). The mechanical properties were inevitably affected by the foaming, but a remarkable reduction down to 30% of the original value of the thermal conductivity was achieved. Morphological analysis by scanning electron microscopy showed a continuous interface between the epoxy GFRP and the foamed layer. © 2018 The Authors. Journal of Applied Polymer Science published by Wiley Periodicals, Inc. J. Appl. Polym. Sci. **2018**, *135*, 46864.

KEYWORDS: epoxy foams; glass fibre reinforced polymers; thermal insulation

Received 9 May 2018; accepted 13 June 2018

DOI: 10.1002/app.46864

INTRODUCTION

Polymer matrix composites (PMCs) are becoming more widely diffused in the Oil & Gas industry. The potential to exploit their outstanding mechanical properties, along with their reduced density compared to metals, makes them a suitable alternative to overcome the technical limitations of traditional structural alloys for deep-water fossil fuels recovery.[1]

One of the issues affecting offshore oil recovery is the need to keep the extracted crude in a fluid state to avoid clogging or solid-phases precipitation, despite the low temperature of ocean water (4 °C on average, can be even lower in particular conditions). There are different techniques to maintain the fluid at the optimal condition, but passive thermal insulation (applied to the pipelines) is one of the most convenient. Thermal insulation is not only a technical requirement but can deeply affect the energy efficiency of the extraction process. On this side, PMCs are already a step ahead compared to metal alloys, thanks to their overall lower thermal conductivity.[2,3]

Their insulation performance can be further improved by the addition of polymer foam liners to the pipe layered structure. Several thermoplastic polymers have been developed in the format of low-density foams, from simple polystyrene and polyurethane, up to high-performance polymers as poly(vinylidene fluoride),[4,5] and are already used in commercial products. The drawback of using these foams is that they have usually poor adhesion properties to thermoset matrix composite substrates, unless advanced adhesive techniques or surface treatment are involved.[6]

The development of foams obtained from thermosetting epoxy resins has followed different routes, due to their different processability. For this class of polymer, there has been a major development of syntactic foams, which can be considered a sort of particulate composite, where hollow spheres are introduced in the resin before curing in order to generate controlled porosity distribution.[7] Epoxy foams are interesting for composite structural application as they have the attitude to adhere effectively to many substrates, show good mechanical properties and are thermally and chemically stable.[8]

Another positive feature of the introduction of foam in the pipe structure is that it does reduce the overall density of the structure. This can play a relevant role in an offshore riser system, which often has to withstand high structural tensile loads[1] and needs additional external buoyancy to achieve a steady structure. The possibility to design the foam layer to be introduced, to achieve a buoyant indifferent pipeline, would greatly ease the designer work, relieving important stresses to the components and materials involved, and increasing the

†Present address: AMPnP Consultants Limited, Richmond TW10 6PQ, Surrey, United Kingdom.

versatility of these pipeline systems. For reference, the main design constraints required to an insulating material for a component such as an offshore deep-water riser for oil recovery are a wide operative temperature range (exceeding 100 °C), a compressive strength able to withstand the high hydrostatic pressure and a very low thermal conductivity (below 0.2 W m^{-1} K^{-1}), as reported in literature.[9]

Other sectors of interest for the polymer insulating materials are the maritime industry in general, the military for submarine vehicles and the oceanographic one for deep-water explorations. A promising application is the use of PMCs to harvest the renewable energy generated by offshore marine currents and tides.[9]

The industry is interested in developing systems where the foaming agent does not involve the use of hazardous chemicals and requires just to introduce simple alteration to the resin curing routine. There are reports in the literature where the foaming agent for epoxy is introduced as an additive in the resin formulation and releases a blowing gas simultaneously with the curing reaction, exploiting the same curing agent and polymerization heat generated.[8,10] By adjusting the resin formulations and the curing parameters, it is possible to obtain foams of different morphologies, with low apparent density.

In this article, we have investigated the formulations and curing parameters to obtain an epoxy foam to be used as thermal insulator layer for a glass fiber reinforced polymer (GFRP). The interfaces with a polymer composite have been evaluated by microscopy and the foam was fully characterized. In particular, in this work, a commercial epoxy resin was used to which a siloxane was added as chemical foaming agent (CFA).[8] During thermal curing, the siloxane reacts with the amine hardener and gaseous hydrogen is released, therefore the foaming occurs simultaneously with the epoxy crosslinking through the amine groups. Different amounts of CFA were attempted in the formulations, between 1 and 5 wt %, to find the optimum for the foam morphology sought. Once the preferred curing route was defined, representative samples were manufactured. The specimens so obtained underwent mechanical testing as quasi-static compression and flexural 3-point bending (3PB). The physical properties were evaluated through dynamic mechanical thermal analysis (DMTA), thermogravimetric analysis (TGA) and thermal conductivity. Microscopic analyses were also performed to investigate the foam microstructure and the interface between the foam and the GFRP.

EXPERIMENTAL

Materials

The two-component *Ampreg 26* epoxy resin with amine hardener, supplied by Gurit (Switzerland), was used as the matrix. The epoxy resin consists of a blend of bisphenol A (50–100%), bisphenol F (25–50%), and 1,6 hexanediol diglycidyl ether (2.5–10%), while the hardener is a blend of amines [polyoxyalkyleneamine (25–50%), 2,2′-dimethyl-4,4′methylenebis(cyclohexylamine) (10–25%), 4,4′-methylenebis(cyclohexylamine) (10–25%), and 2,2′iminodiethylamine (2.5–10%)]. Bulk epoxy samples were prepared by compression molding with a 24 h room temperature curing, followed by a postcure at 80 °C for 5 h.

The CFA is the 1,1,3,3-tetramethyl disiloxane. It was purchased from Sigma Aldrich (St. Louis, MO) and used as received.

The glass fiber unidirectional fabric, supplied by Gammatensor (Spain), was made of SE 2020 Direct Roving comprising of Advantex glass (boron free) E-CR glass fibers, which are specifically designed for the production of noncrimped fabrics and have a proprietary sizing which is specifically designed for excellent adhesion with epoxy resin systems. The vacuum bag technique was used to produce the GFRP, followed by a postcure at 80 °C for 5 h, following the supplier specification data sheet.

Preparation of the Epoxy Foam

The epoxy foam was prepared following a method reported in literature,[8] evaluating mixing times in order to find the most suitable conditions to obtain an uniform foaming in the resin. To avoid the early CFA reaction, due to the rather long gel time of the epoxy resin at room temperature (about 4 h), the CFA is added to the mixture after a precuring period of 2 h. Therefore, the epoxy resin was mixed with the amine hardener (epoxy/hardener ratio 100:33) and left to rest for about 2 h at room temperature. While the viscosity was still low, the 1,1,3,3-tetramethyldisiloxane, was added to a content of 1–5 wt %, with respect to the epoxy plus hardener mass, and mixed manually. The viscous liquid prefoam is then poured into the assembled mold and left to rest for other 2 h reaching complete gelification. Skipping this step and introducing the resin directly to thermal postcuring, would induce an abrupt decrease of viscosity of the resin due to the higher temperature, causing the coalescence and escape of most of the bubbles generated. A final thermal curing was obtained by exposing the sample at 80 °C for 5 h. During the postcure, further foaming happens with a volume increase to 200%. Foam samples were also cured as a top layer of GFRP flat panels, following the same procedure reported above.

Characterization

The apparent density was measured following the American Society for Testing and Materials (ASTM) D1622M. DMTA, using 3PB loading mode, were performed using an RSA 3 analyzer, by TA Instruments, to evaluate the glass-transition temperature (T_g). The temperature ramp was set from 25 up to 150 °C, at 5 °C min^{-1} heating rate. The thermal stability and degradation were evaluated by TGA, performed with a NETZSCH (Germany) TG 209 F1 *Libra*. A 10 °C min^{-1} heating ramp, up to 450 °C was employed.

Mechanical testing as quasi-static compression (following ASTM D695, for the bulk epoxy, and D1621, for the foam) and flexural 3PB test (ASTM D790, for bulk epoxy, and ISO 1209, for the foam) were performed using a Zwick Roell (Germany) Z50 universal testing machine.

Thermal conductivity tests were performed using two different experimental setups:

- A TPS 2500 S instrument by Hot Disk AB (Sweden), following the ASTM C177, to evaluate different foam formulations at room temperature.
- A Fox 50 Heat Flow Meter by TA Instruments, following the ASTM C518. The thermal conductivity was evaluated at different equilibrium temperatures up to 70 °C.

Porosity distribution and the quality of the adhesion of the foam to the GFRP substrates were evaluated by field-emission SEM (FESEM SupraTM 40, Zeiss, Oberkochen, Germany) equipped

with energy-dispersive X-ray spectroscopy (EDAX PV 9900). The samples were sputter-coated with gold prior to the analysis and inspected at an accelerating voltage of 15 kV. The pore size dimensions were evaluated from the acquired cross-sectional images using the ImageJ image processing software.[11] Values obtained by image analysis were converted to 3D values using the stereological equation $D_{pore} = D_{hole}/0.785$, in order to determine the effective pore size.[12]

RESULTS AND DISCUSSION

Foaming Process

Many factors contribute to the foaming reaction; the main ones are the temperature of the mixed resin, directly influenced by the curing heat released, and the amount of the CFA added. The viscosity of the resin is critical for the proper foaming process, and the curing kinetics can abruptly change the gelification process, posing a relevant processing difficulty. As reported in literature,[13,14] the optimal viscosity range to obtain a narrow pore size distribution is obtained at the gel point. A controlled pore size ensures consistent foam quality and improved mechanical properties. An early foaming gas release will lead to coalescence and escape of the bubbles due to the low viscosity of the resin; a delayed release will result in an insufficient or inhomogeneous foaming.[13] In our case, we defined the maximum amount of CFA at 5 wt %, above which the bubble formation was uncontrolled. A proper formulation procedure was established, as reported in the "Experimental" section.

The foamed samples obtained by increasing the CFA content in the formulations were characterized both for mechanical and thermal properties. Samples of the epoxy foams obtained with the addition of increasing siloxane content, from 1 to 5 wt % are shown in Figure 1. In Figure 2, the foam density as a function of CFA content is reported; as expected an important decrease in the apparent density was achieved, from 1.2 g cm^{-3} for the bulk epoxy material down to 0.4 g cm^{-3} for the foam synthesized with the addition of 5 wt % of CFA.

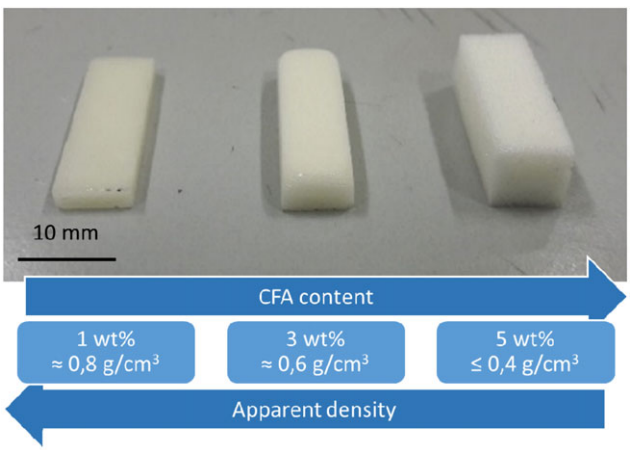

Figure 1. Epoxy foams obtained by the addition of increasing content of siloxane CFA from 1 to 5 wt %. [Color figure can be viewed at wileyonlinelibrary.com]

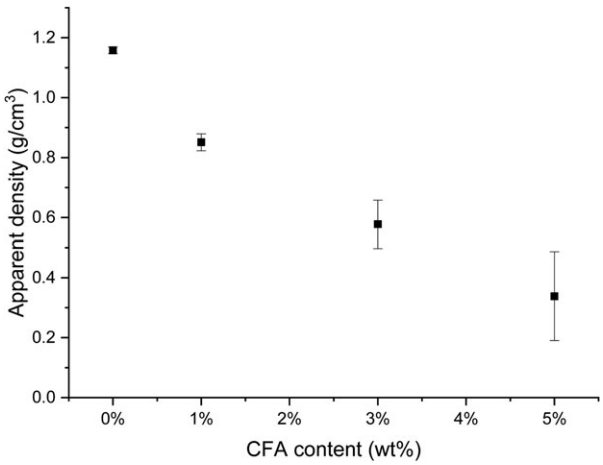

Figure 2. Density of the crosslinked epoxy foam as a function of CFA content.

Thermal Characterization

Thermomechanical properties were measured by DMTA and the glass-transition temperature (T_g) of the crosslinked bulk epoxy and foams was determined as the peak of tan δ curves. The average T_g data are listed in Table I. It is possible to observe that the foam formation did not significantly affect the ultimate thermomechanical properties of the crosslinked epoxy network and the T_g was not altered by the foam formation. Similar behavior was previously reported in literature for epoxy foams.[8]

TGA was performed to compare the thermal degradation among the different formulations. The TGA curves did not reveal any significant effect towards the thermal stability of the foams compared to the bulk epoxy. This was an important result because it is fundamental that the foam should not influence the high thermal stability of the epoxy material. The epoxy starts to degrade at around 300 °C, the temperature at 5 wt % mass loss are reported in Table I (T5%). A slight increase in char content was also evidenced by increasing the CFA content in the formulation. This was attributed to the siloxane molecule used as CFA.

Table I. Thermal Properties of Crosslinked Epoxy Bulk and Foam Materials

wt % CFA	T_g[a] (°C)	T5%[b] (°C)	Char content[c] (wt %)
0	98 ± 1	300	7
1	97 ± 2	300	8
3	96 ± 3	298	9
5	97 ± 3	296	11

CFA, chemical foaming agent; DMTA, dynamic mechanical thermal analysis; TGA, thermal gravimetric analysis.
[a] Determined as the peak of tan δ of DMTA curves.
[b] Determined by TGA, as the temperature at which there is a measurable 5 wt % loss.
[c] Determined by TGA as the residual sample mass.

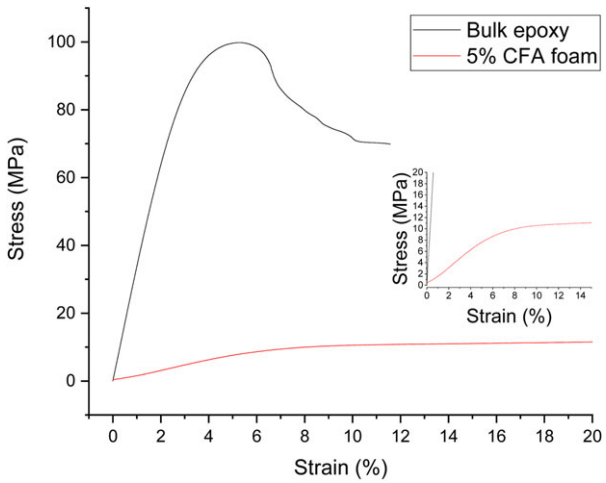

Figure 3. Typical stress–strain curves for epoxy bulk and foam samples from the unidirectional compression test. [Color figure can be viewed at wileyonlinelibrary.com]

Mechanical Characterization

The 5 wt % CFA foam is the most promising formulation for the lower apparent density achievable, hence greater expected thermal insulation. For this reason, the mechanical characterization focused on crosslinked epoxy foams obtained by this formulation. Quasi-static compression (Figure 3) and 3PB (Figure 4) mechanical tests were performed on different batches of the foam. To compare the performance, bulk epoxy specimens were tested in the same loading configurations. Characterizing materials with such different morphologies is not a trivial task, as their mechanical properties can vary in a very large extent and in this case the applicable test standards are different.

During the compression test, none of the foam samples failed (meaning as they did not crack or explode); hence, the run is ended at 25% of nominal strain. The deformation mainly happens by barreling and crushing of the porosity, with an increase of the apparent density. The bulk epoxy specimens tend to buckle instead, and the tests were interrupted after the maximum stress was reached, around 6% of strain.

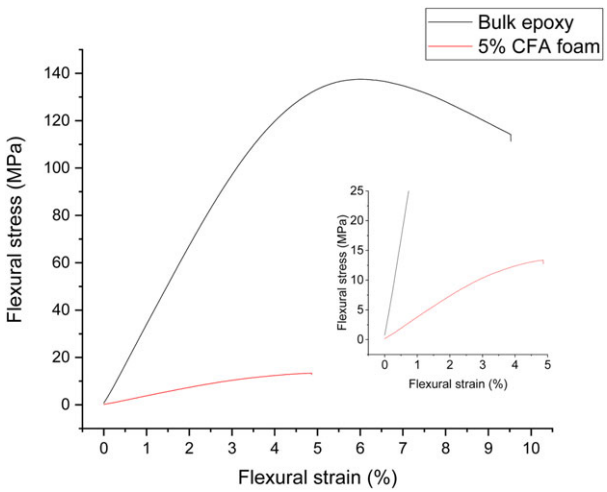

Figure 4. Typical stress–strain curves for epoxy bulk and foam from the 3PB test. [Color figure can be viewed at wileyonlinelibrary.com]

In the flexural test, the epoxy foam showed a fairly brittle behavior, failing just below 5% of flexural strain. The bulk epoxy well exceeded this value, allowing a good amount of plastic deformation before failure. The strength of the bulk epoxy was evaluated at 5% of strain, as prescribed by the standard.

To compare the mechanical performance of different materials, it is useful to consider some of their physical properties, which become relevant for such design where lightweight can be critical. This is typical in aerospace and transport engineering design, but it can be relevant to other structural applications. To better appreciate the opportunity offered by materials with very different characteristics, performance indices were introduced, such as specific elastic modulus and strength, which are the ratio of the mechanical properties and the material density (see eq. (1)). These facilitate the selection for a design of a component where, for example, both stiffness and weight need to be optimized. As it can be found in the literature, simple mechanical theory assumptions lead to the definition of further indices in function of the relative main loading mode experienced by the component.[15]

$$\frac{E}{\rho}=\frac{\text{elastic modulus}}{\text{apparent density}}$$

$$\frac{\sigma}{\rho}=\frac{\text{critical stress}}{\text{apparent density}} \quad (1)$$

In Table II, along with Young's modulus (E) and the ultimate strength (σ), we collected some of these indices when compressive loads are involved. In Table III, the same indices are presented, relatively to flexural load. The indices help to evaluate the more suitable material considering the required stiffness or the most likely failure cause.

From the data collected, it can be highlighted how the foam apparent density, has a deep influence on the resulting mechanical properties, not matching the performance of the bulk material. When loaded in unidirectional compression, it appears that the foam has a lower elastic modulus than in bending, where a mixed tension/compression stress state is experienced by the material. The properties found for this foam formulation are in agreement or even slightly superior to the values reported in literature.[13,16,17]

Thermal Conductivity

Foamed epoxy samples, obtained with different CFA content, were prepared to evaluate the effect of the apparent density on the thermal conductivity. The obtained values are reported in Figure 5. As expected, a noticeable decrease of thermal conductivity is measured for the less dense foams, thanks to the increasing amount of CFA introduced in the formulation. The thermal conductivity decreased from 0.24 W m^{-1} K^{-1} for the bulk crosslinked epoxy resin down to 0.07 W m^{-1} K^{-1} for the crosslinked foams obtained adding 5 wt % of CFA. The large decrease of the thermal conductivity by decreasing polymer density can be addressed to the lower proportion of solid epoxy and the increased air volume fraction, which is characterized by a much

Table II. Mechanical Properties in Compression for Bulk and Foamed Epoxy

Material	ρ (kg m^{-3})	Comp. E (MPa)	E/ρ (MPa m^{-3} kg^{-1})	Comp. σ (MPa)	σ/ρ (MPa m^{-3} kg^{-1})
Bulk epoxy	1150 ± 10	3330 ± 84	2.895	100.5 ± 1.1	0.087
5% CFA foam	400 ± 20	155 ± 3	0.386	10.4 ± 0.2	0.026

CFA, chemical foaming agent.

Table III. Mechanical Properties in Flexure Between Bulk and Foamed Epoxy

Material	ρ (g cm^{-3})	Flex. E (MPa)	E/ρ (MPa m^{-3} kg^{-1})	Flex. σ (MPa)	σ/ρ (MPa m^{-3} kg^{-1})
Bulk epoxy	1150 ± 10	3404 ± 55	2.948	132.3 ± 1.1	0.115
5% CFA foam	400 ± 20	378 ± 7	0.941	12.6 ± 0.6	0.031

CFA, chemical foaming agent.

lower thermal conductivity (0.026 W m^{-1} K^{-1}) compared to the epoxy polymer.[18]

Due to foaming and, hence, increase in the apparent density, there is a decrease by 70% of the original bulk epoxy conductivity. An analytical model to evaluate the conductivity of closed-cellular structures was proposed by Ashby.[19] Taking into account only thermal conduction as heat transfer mechanism, it relates the conductivity to the relative density (ρ_r) of the material, meant as the ratio between the apparent density of the foam and the one of the bulk polymer, as reported in eq. (2):

$$\lambda_{foam} = \frac{1}{3}\left(\rho_r + 2\rho_r^{3/2}\right)\lambda_{epoxy} + (1-\rho_r)\lambda_{air} \quad (2)$$

It seems that the model slightly overestimates the foam conductivity, but there is a satisfactory agreement with the experimental data. These results support the use of foamed polymer as a way to improve the pipeline insulation performance.

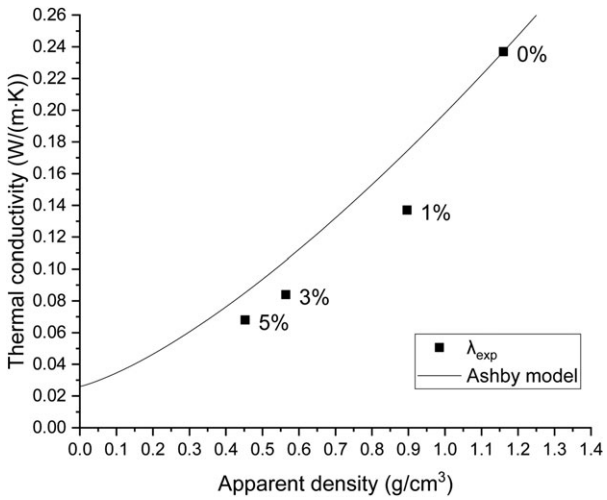

Figure 5. Foam thermal conductivity of bulk epoxy and foams at 25 °C in relation to its apparent density. The percentages indicate the foaming agent wt % added to the relative foam formulation.

We also investigated the foam thermal conductivity in relation to the environment temperature, to evaluate if it is stable when it comes to the possible different operating scenarios. This test was performed on larger foam disks, obtained from the 5 wt % of foaming agent formulation. Different temperature steps up to 70 °C were run, in order not to enter the glass transition range, as the samples would have been squeezed in between the testing plates, due to the loss in stiffness. This would alter the foam apparent density, and then the results cannot relate to the original material properties. As shown in Figure 6, there is not a large variation in the conductivity value, just a slight linear increase with temperature, as expected. These data show the stability of thermal insulation behavior of the epoxy foams in a large temperature interval.

Morphological Analysis

Micrographs of the cross-sectional surfaces of the epoxy foams were obtained by scanning electron microscopy (SEM). In Figures 7 and 8, the micrographs for the sample obtained in the presence of 1 and 5 wt % of CFA are reported, respectively. The

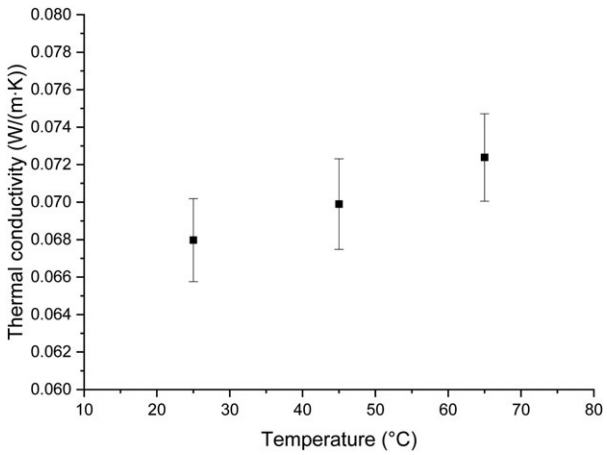

Figure 6. Thermal conductivity at different temperatures in steady state for the epoxy foam (5 wt % FCA).

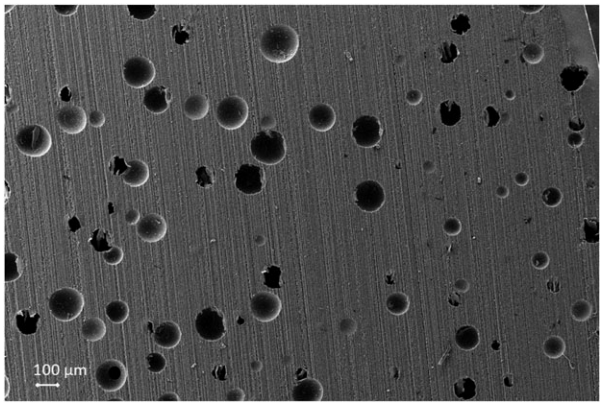

Figure 7. Cross section of a foam sample obtained by adding 1 wt % CFA.

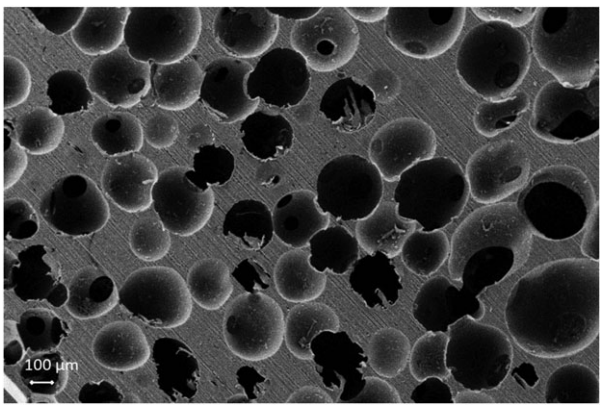

Figure 8. Cross section of a foam sample obtained by adding 5 wt % CFA.

porosity is mainly closed, fairly spherical with an average pore size in the order of the tenths of millimeters.

In Figure 9, the average porosity diameter (calculated from the SEM images) are reported as a function of FCA content. The average diameter increased by increasing the FCA content. This can be attributed to coalescence phenomena, which are favored by an increase on blowing agent concentration. At the end, this leads to a lower apparent density.

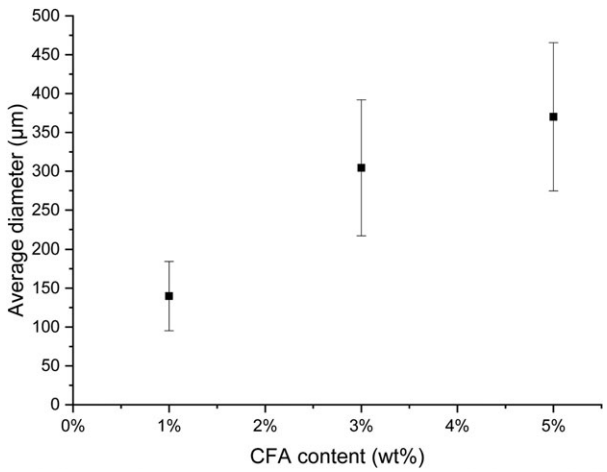

Figure 9. Averaged porosity diameter in relation to the amount of CFA added.

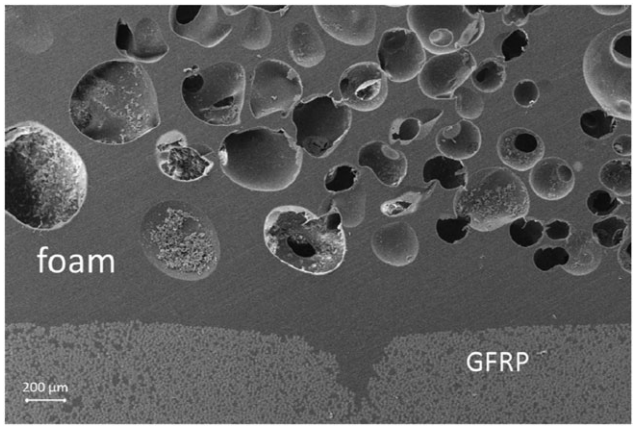

Figure 10. Cross section of the adhesion interface between the foam and a GFRP substrate.

Foamed samples were deposited on GFRP substrates, as described in the "Experimental" section. The interface does not show the presence of defects and it is possible to observe a continuous interface among the epoxy composite (GFRP) and the epoxy foam, even if they were cured at different times (see Figure 10). This confirms the good compatibility of the foam with structural substrates, with a good interface and adhesion properties.

CONCLUSIONS

An epoxy foam was successfully prepared following the synthesis route of adding a CFA during the curing stage of an epoxy resin. This manufacturing approach can be competitive to other foaming processes (e.g., physical foaming, syntactic foams) as it does not involve the use of hazardous chemicals and requires just to slightly modify the resin curing routine, yet it does rely on the sharp transition in the viscosity happening at the gel point.

The foam samples obtained underwent a thorough characterization regarding physical, mechanical and thermal properties. The results show that a relevant decrease of the apparent density of the foam can be obtained by adding up to 5 wt % of CFA. Although the mechanical properties are inevitably affected by the foaming, an interesting reduction down to 30% of the original value of the thermal conductivity can be achieved, while the glass transition and the thermal stability of the material are unaffected.

Microscopic investigation showed a continuous interface among the epoxy GFRP and the foamed layer. This confirms the compatibility of the foam with structural substrates, with a good interface and adhesion properties.

ACKNOWLEDGMENTS

Special thanks go to Samuele Colonna and Alberto Fina from Politecnico di Torino, for the thermal conductivity test performed on the TPS 2500S at the EMC laboratory, in Alessandria (ITA). Special thanks would also go to Cristian Marro, from DISAT department of Politecnico di Torino, for his support in preparing the samples for the SEM analysis. The authors would like to

acknowledge that the project leading to this article has received funding from the European Union's Horizon 2020 Research and Innovation Programme under the Marie Sklodowska-Curie grant agreement No. 642557 (CoACH ETN, http://www.coach-etn.eu/).

REFERENCES

1. M. Vermilyea, V. Jha, J. Latto, D. Finch, T. A. Anderson, N. Dodds, Presented at the Offshore Technology Conference, Houston, TX, **May, 2013**.
2. Davies, P. Behavior of marine composite materials under deep submergence. In Marine Applications of Advanced Fibre-Reinforced Composites; Summerscales, J.; Graham-Jones, J., Eds., Elsevier, Philadelphia, USA, **2016**. p. 125.
3. Sanada, K.; Tada, Y.; Shindo, Y. *Compos. Part A: Appl. Sci. Manuf.* **2009**, *40*, 724.
4. Danowska, M.; Piszczyk, Ł.; Strankowski, M.; Gazda, M.; Haponiuk, J. T. *J. Appl. Polym. Sci.* **2013**, *130*, 2272.
5. Siripurapu, S.; Gay, Y. J.; Royer, J. R.; DeSimone, J. M.; Spontak, R. J.; Khan, S. A. *Polymer*. **2002**, *43*, 5511.
6. Deng, S.; Djukic, L.; Paton, R.; Ye, L. *Compos. Part A: Appl. Sci. Manuf.* **2015**, *68*, 121.
7. Baumeister, E.; Klaeger, S. *Adv. Eng. Mater.* **2003**, *5*, 673.
8. Stefani, P. M.; Barchi, A. T.; Sabugal, J.; Vazquez, A. *J. Appl. Polym. Sci.* **2003**, *90*, 2992.
9. D. Choqueuse, P. Davies, Ageing of composites in underwater applications, In: Ageing of Composites (Ed: Martin R.), Woodhead Publishing, Cambridge UK, **2008**, p 467–498.
10. Alonso, M. V.; Auad, M. L.; Nutt, S. *Compos. Part A: Appl. Sci. Manuf.* **2006**, *37*, 1952.
11. ImageJ, https://imagej.nih.gov/ij/ (accessed February, 2018).
12. Strozi Cilla, M.; Colombo, P.; Raymundo Morelli, M. *Ceram. Int.* **2014**, *40*, 5723.
13. Chen, B.Y.; Wang, Y.S.; Mi, H.Y.; Yu, P.; Kuang, T.R.; Peng, X.F.; Wen, J.S. *J. Appl. Polym. Sci.* **2014**, *131*, 41181.
14. Takiguchi, O.; Ishikawa, D.; Sugimoto, M.; Taniguchi, T.; Koyama, K. *J. Appl. Polym. Sci.* **2008**, *110*, 657.
15. Ashby, M. Materials Selection in Mechanical Design. 4th ed.; Butterworth-Heinemann, Elsevier, Waltham, USA. **2011**.
16. Stefani, P. M.; Cyras, V.; Tejeira Barchi, A.; Vazquez, A. *J. Appl. Polym. Sci.* **2006**, *99*, 2957.
17. Ren, Q.; Xu, H.; Yu, Q.; Zhu, S. *Ind. Eng. Chem. Res.* **2015**, *54*, 11056.
18. Forest, C.; Chaumont, P.; Cassagnau, P.; Swoboda, B.; Sonntag, P. *Prog. Polym. Sci.* **2015**, *41*, 122.
19. Ashby, M. F. Cellular solids - scaling of properties. In Cellular Ceramics; Scheffler, M.; Colombo, P., Eds., Weinheim, Germany: Wiley-VCH, **2006**. p. 1.